doi:10.1111/evo.13815

Head-turning morphologies: Evolution of shape diversity in the mammalian atlas–axis complex

Abby Vander Linden,[1] Kristin M. Campbell,[2] Erin K. Bryar,[2] and Sharlene E. Santana[2,3,4]

[1]*Graduate Program in Organismic and Evolutionary Biology, University of Massachusetts Amherst, Amherst, Massachusetts*

[2]*Department of Biology, University of Washington, Seattle, Washington*

[3]*Burke Museum of Natural History and Culture, Seattle, Washington*

[4]*E-mail: ssantana@uw.edu*

Received February 13, 2019
Accepted July 1, 2019

Mammals flex, extend, and rotate their spines as they perform behaviors critical for survival, such as foraging, consuming prey, locomoting, and interacting with conspecifics or predators. The atlas–axis complex is a mammalian innovation that allows precise head movements during these behaviors. Although morphological variation in other vertebral regions has been linked to ecological differences in mammals, less is known about morphological specialization in the cervical vertebrae, which are developmentally constrained in number but highly variable in size and shape. Here, we present the first phylogenetic comparative study of the atlas–axis complex across mammals. We used spherical harmonics to quantify 3D shape variation of the atlas and axis across a diverse sample of species, and performed phylogenetic analyses to investigate if vertebral shape is associated with body size, locomotion, and diet. We found that differences in atlas and axis shape are partly explained by phylogeny, and that mammalian subclades differ in morphological disparity. Atlas and axis shape diversity is associated with differences in body size and locomotion; large terrestrial mammals have craniocaudally elongated vertebrae, whereas smaller mammals and aquatic mammals have more compressed vertebrae. These results provide a foundation for investigating functional hypotheses underlying the evolution of neck morphologies across mammals.

KEY WORDS: **Cervical vertebrae, mammals, morphology, locomotion, spherical harmonics analysis.**

Clade-wide evolutionary analyses of anatomical structures have proven fruitful in understanding the ecological pressures that shape morphological diversity (e.g., Felice and Goswami 2018; Slater and Friscia 2019). The radiation of mammals and its accompanying morphological and ecological diversity provides a rich opportunity for exploring macroevolutionary patterns in form and function and their potential adaptive significance. For example, the morphology of mammal skulls, teeth, jaws, and limbs have been shaped by demands for efficient food processing, locomotion, and combat (e.g., Coombs 1983; Van Valkenburgh 1985; Popowics and Fortelius 1997; Pérez-Barbería and Gordon 1999; Caro et al. 2003; Clauss et al. 2008; Polly 2008; Santana et al. 2010; Goswami et al. 2011). Conversely, the evolution of body size in mammals has also created structural and mechanical constraints that influence the morphospace within which the mammalian skeleton can evolve (Gould 1966; Jungers 1984; Christiansen 2002; Cardini and Polly 2013; Arnold et al. 2017).

Relative to the skull and limbs, the macroevolution of the spinal skeleton has been greatly understudied in mammals; most comparative work has focused on the morphology of thoracic and lumbar vertebrae only within individual families (e.g., Johnson and Shapiro 1998; Shapiro and Simons 2002; Pierce et al. 2011; Granatosky et al. 2014). The evolution of functional and morphological diversity in the mammalian cervical spine generally, and the atlas–axis complex in particular, has received less attention, even though the atlas–axis complex is a major skeletal innovation

in mammalian evolution (Evans 1939). These first two cervical vertebrae represent a simplification of the vertebral morphologies found in nonmammalian synapsids (Sidor 2001), and allow for a greater variety and range of head movements and postures than those available to any mammalian ancestor (Evans 1939; Kemp 1969; Crompton and Jenkins 1973). The articulation of the mammalian atlas with two occipital condyles in the skull allows flexion and extension of the head with less strain of the spinal cord than when a single occipital condyle is present, as in reptiles (Crompton and Jenkins 1973). Although the atlanto-occipital joint enables flexion and extension, the peg-like dens of the axis acts as a pivot about which the atlas and head rotate laterally (Evans 1939). As a consequence, the atlas–axis complex allows mammals to decouple these motions, and to more precisely perform behaviors critical for survival, such as subduing, killing, and biting prey (Van Valkenburgh and Ruff 1987; Ydesen et al. 2014); elevating and depressing the head for grazing, gnawing, or digging (Pellis and Officer 1987; Du Toit 1990; Reichman and Smith 1990; Lessa et al. 2008; Zsoldos and Licka 2015); and combating conspecifics (Kitchener 1988; Stankowich 2012). Consistent with their functional roles, the atlas and axis appear to exhibit broad morphological diversity across mammals.

Little is known about the factors underlying the morphological diversity and evolutionary patterns of the atlas and axis vertebrae across extant mammals; previous studies have focused on examining morphological transitions in extinct taxa (Jenkins 1960; Kemp 1969; Kikuchi et al. 2012), or on comparing atlas and/or axis morphologies within specialized groups of mammals (e.g., primates, tree shrews, felids; Sargis 2001; Manfreda et al. 2006; Randau et al. 2016a, 2016b; Nalley and Grider-Potter 2017). Comparative studies of atlas shape have found contrasting trends across the mammal groups studied to date. Atlas shape has been linked to changes in body size and the evolution of bipedal posture in primates (Manfreda et al. 2006), but a study in felids found that atlas shape was related to body size but not to diet or locomotor ecology (Randau et al. 2016a, 2016b). Within Euarchontogliran mammals, including primates and rodents, atlas shape is associated with body size, but not with head size or locomotion (Vander Linden et al. 2019). Furthermore, because almost all mammals, from giraffes to humans, possess seven cervical vertebrae (Narita and Kuratani 2005), it has been proposed that the extensive variation in neck length is mainly due to scaling and shape changes within individual vertebrae (Arnold et al. 2017). However, no quantitative studies have tested this idea nor the relative importance of different behaviors (e.g., feeding or locomotion) on the evolution of atlas and axis diversity across mammals.

Given the functional and evolutionary importance of the mammalian atlas–axis complex, we aim to investigate its morphological diversity and evolution within the context of variation in body size, diet, and ecology across Mammalia. First, we hypothesize that the shape of these two vertebrae exhibits an allometric relationship with body mass, such that larger-bodied mammals have relatively more robust vertebrae that would support increased skull weight while providing larger attachment surfaces for larger neck muscles (Manfreda et al. 2006). Second, we hypothesize that behaviors associated with consuming animal prey (killing, shaking, tearing, etc.) as opposed to plant material (browsing and grazing) impose different mechanical demands on the neck of carnivores versus herbivores and omnivores, resulting in the evolution of different atlas and axis morphologies across species with different diets. We expect to find shorter, more compressed vertebrae with larger transverse and spinous processes in carnivores, which would allow for a greater range of neck movements and provide larger attachment areas for powerful neck muscles (Pierce et al. 2011). Third, we hypothesize that mechanical demands of different locomotor modes require different degrees of head support, neck rotation, and flexibility. Therefore, we expect to find shorter vertebrae with more surface for rotation of the axis and flexion/extension of the head in climbing/gliding taxa when compared to terrestrial taxa. As these three hypotheses are not mutually exclusive, we explore whether models with single factors or combinations of body size, diet, and locomotion better explain the observed diversity in atlas and axis morphology. Alternatively, evolutionary history might explain most of the diversity in atlas and axis shape (Randau et al. 2016a). We use phylogenetic comparative methods and spherical harmonics analyses to quantify and compare the three-dimensional shape of vertebrae, and test whether evolutionary changes in their morphology are associated with differences in body size, diet, and locomotion across the mammal phylogeny.

Materials and Methods

SAMPLING AND ECOLOGICAL DATA

All specimens included in this study were obtained from the Burke Museum of Natural History and Culture (University of Washington, Seattle, WA; Table S1). We sampled one atlas and one axis vertebra from 80 species of mammals, with each species belonging to a different family across all orders. This sample included representative species from families within the orders Monotremata and Marsupialia and the superoders Laurasiatheria, Euarchontoglires, Afrotheria, and Xenarthra (Meredith et al. 2011). To minimize any effect of sexual dimorphism, we used adult female specimens except in a few cases where only adult males were available. We incorporated phylogenetic relationships and divergence times between taxa using a time-calibrated family-level molecular tree of Mammalia published by Meredith et al. (2011) and pruned to our study species (Fig. S1 and Table S2).

We sourced body mass data for each species from the PanTHERIA dataset (Jones et al. 2009) using the Wilson and Reeder (2005) taxonomy, and $\log_{10}$-transformed these data to improve normality for statistical analyses. Using the Kissling et al. (2014) mammal diet dataset, we assigned each species to one of the following diet categories: carnivore (consuming predominantly invertebrate or vertebrate animals), herbivore (consuming predominantly plant material, including leaves, stems, roots, seeds, fruits, nectar, or other plant parts), or omnivore (consuming both plants and animals). We assigned species to one of three locomotor categories based on literature accounts (Table S1 and Supporting Information References): (1) aquatic—fully aquatic species such as whales and dolphins, as well as species that primarily locomote and forage in water such as seals and walruses; (2) ground—any species with primarily terrestrial, semi-fossorial, or fossorial locomotion, including semi-aquatic species that also spend a substantial amount of time foraging and traveling on land, such as the capybara; and (3) above ground—species that use scansorial or primarily arboreal locomotion and species that glide or fly. We opted to group fossorial and terrestrial species, as well as arboreal and gliding/volant species, to achieve sufficient sample sizes within groups for meaningful statistical analyses while capturing broad similarities in locomotor mode.

Some species included in our study have fused portions of the cervical vertebral column, resulting in a syncervical anatomy (Vanburen and Evans 2016). In species with a fused atlas and axis (C1-C2; the whale *Berardius bardii* and dolphin *Lagenorhynchus obliquidens*), we opted to treat the syncervical as analogous to the atlas, considering it a first functional unit of the cervical spine. In species with fused vertebrae caudal to the atlas (the porcupine *Erethizon dorsatum* C2-C3, kangaroo rat *Dipodomys microps* C2-C3, and armadillo *Dasypus novemcinctus* C2-C4), we treated the fused vertebrae as analogous to the axis or a second functional unit.

3D IMAGING

We used both laser scanning and micro-computed tomography (μCT) scanning to generate 3D models of vertebrae. We scanned specimens >5 cm in diameter using a NextEngine HD laser scanner (NextEngine, Inc., Santa Monica, CA). We scanned each vertebra in two orientations, resulting in 12 partial scans spanning 360°. We then aligned and merged the partial scans using the NextEngine Scan Studio software, and exported *.STL (surface) files for postprocessing. For specimens too small to be imaged by the laser scanner, we used a Skyscan 1174 μCT scanner (Bruker MicroCT, Belgium). We used a 0.25 mm Al filter, a voltage of 50 kV, and a current of 800 uA for all μCT scans. Voxel sizes ranged from 9 to 30 μm, depending on specimen size. We reconstructed μCT scans as image stacks (slices) in NRecon version 1.6.9.18 (Bruker microCT), and automatically segmented pixels representing bone in Mimics 17.0 (Materialise, Belgium). We then rendered these as 3D objects, and exported them as *.STL files.

We used Geomagic Studio 14.0 (3D Systems, Inc., Rock Hill, CA) to process all STLs prior to spherical harmonics (SPHARM) analyses. We removed floating polygons, automatically filled small holes, and deleted polygons representing internal trabeculae in models generated from μCT scans to create a watertight surface mesh (Fig. 1A). Because SPHARM requires united objects with no holes (Shen et al. 2009), we filled the transverse foramina and vertebral foramina of all vertebrae using Geomagic algorithms that automatically fill holes following the curvature of the surface, thus preserving the shape of the mesh. All meshes were then automatically resurfaced to improve triangle quality and reduced to 20,000 triangles (Fig. 1B).

SPHERICAL HARMONICS ANALYSES

We performed separate SPHARM analyses of the atlas and axis datasets using the SPHARM 2.0 (Shen et al. 2009) software in Matlab R2014a (The Mathworks, Inc., Natick, MA). Six landmarks on each vertebra were used to reorient, rescale, and reposition (i.e., register) the models within each dataset (Fig. 1B; see Table S3 for landmark descriptions). Following McPeek et al. (2008), we resized all meshes to a centroid size of 1, and registered them to a template model using the 3D landmarks. We selected for the SPHARM algorithm to model the vertebrae using 15° of smoothing, resulting in an output of 768 spherical harmonics coefficients for each model (McPeek et al. 2008) (Fig. 1C).

STATISTICAL ANALYSES

To reduce the dimensionality of the spherical harmonics coefficients dataset and determine the major axes of morphological variation, we performed a principal component analysis (PCA) of the spherical harmonics coefficients for each species in both the atlas and axis datasets in R 3.3.3, using the *prcomp* function in the base R library (R Core Team 2018). Because the spherical harmonics coefficients are complex numbers, the PC scores for each species were also complex numbers. However, the complex portions of the scores were either 0 or very close to 0, so we discarded the complex portions of the numbers before using the PC scores in subsequent analyses (following McPeek et al. 2009). The first two PCs in both the atlas and axis datasets accounted for over 50% of the total variance, with all other PCs accounting for less than 7% each (Table S4). To visualize shape change across the mammalian atlas and axis morphospaces, we used the SPHARM software to generate "eigenshapes," or spherical harmonics models representing the average vertebral shape and the vertebral shapes at ±2 standard deviations from the average along each PC axis (McPeek et al. 2009) (Fig. 2).

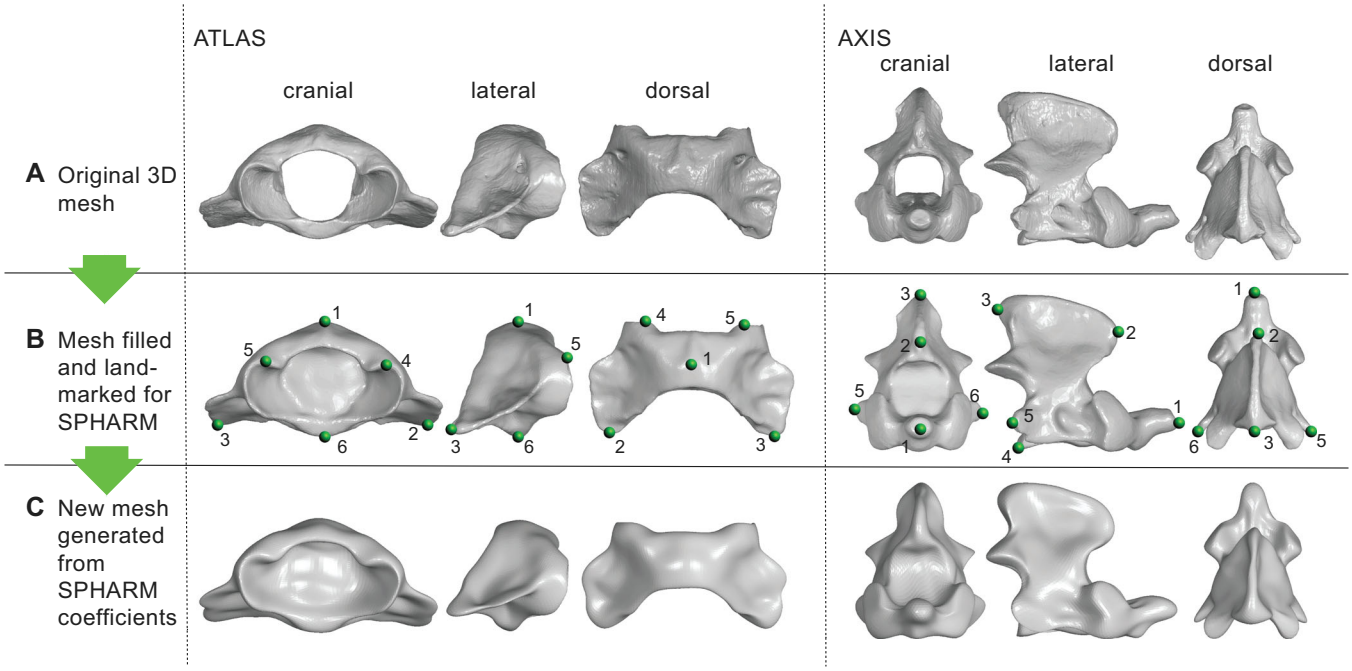

Figure 1. **Illustration of atlas and axis morphology of an example specimen (*Pteropus poliocephalus*, the gray-headed flying fox) and the SPHARM modeling process. (A) A 3D mesh is generated from μCT or laser scan data. (B) The transverse foramina and vertebral foramina are filled using automatic hole-filling algorithms and the mesh is reduced to exactly 20,000 triangles. 3D coordinates for six landmarks are recorded for each specimen; numbers refer to landmark descriptions in Table S3. (C) Once all meshes have been prepared and landmarked, a random mesh is chosen as a template in the SPHARM software and all other models are registered to the template using the landmarks. The SPHARM algorithm then calculates the spherical harmonics coefficients for each specimen and generates a new mesh that visually represents those coefficients. The SPHARM coefficients are then used for further analyses.**

To estimate the effect of shared evolutionary history, we used the *phytools* package in R (Revell 2012) to calculate Blomberg's K statistic for all 80 PCs of the atlas and axis datasets, respectively. For all phylogenetic analyses, we incorporated tree topology and branch length information from the Meredith et al. (2011) phylogeny. We tested for significant differences between the estimated K value and 0 (no phylogenetic signal) using 1000 random permutations of the data (Revell 2012). We used the morphol.disparity function in the *geomorph* R package (Adams and Otárola-Castillo 2013) to estimate multivariate shape disparity across major mammal clades. We estimated shape disparity as Procrustes variance in PC scores from all 80 PC axes between the six mammalian clades for both the atlas and axis datasets. We tested for pairwise differences in disparity between groups using 1000 random permutations of the residuals.

We examined the relationship among atlas and axis shape and body size, diet, and locomotor ecology across mammals via phylogenetic generalized least squares (PGLS) regressions conducted with the *caper* package in R (Orme et al. 2013). The full model for both atlas and axis analyses included $\log_{10}$-transformed body mass, diet, and locomotion categories for each species as predictors of the PC scores for each principal components axis analyzed. We used a maximum-likelihood (ML) estimate of Pagel's lambda to scale the branch lengths of the underlying phylogenetic variance–covariance matrix in each PGLS regression (Pagel 1999). Using the *MuMIn* package in R (Bartoń 2016), we compared Akaike information criterion (AICc) values corrected for small sample sizes of models including all possible combinations of predictor variables. We considered models with ΔAICc > 2 to be best supported by the data (Burnham et al. 2011). Because the *caper* PGLS function requires a univariate response variable, and because each of our PC axes represents distinct and interpretable morphological trends, we analyzed each PC separately. We initially conducted AIC model comparisons for the effects of our predictor variables on PC 1–5 (>70% of shape variation) for both the atlas and axis datasets. However, we found the model comparison results for PC3, PC4, and PC5 to be uninformative, as all models either had very similar AIC scores, or were simply supported in order of increasing model complexity, with the best model being just the response variable. Therefore, we report the PGLS analyses and phylogenetic signal for PC1 and PC2 (but see Table S5 for results of PCs 3–5).

PGLS models with a combination of continuous and categorical predictor variables are difficult to represent graphically. To visualize trends in vertebra shape between diet and locomotor categories, we generated boxplots of PC1 and PC2

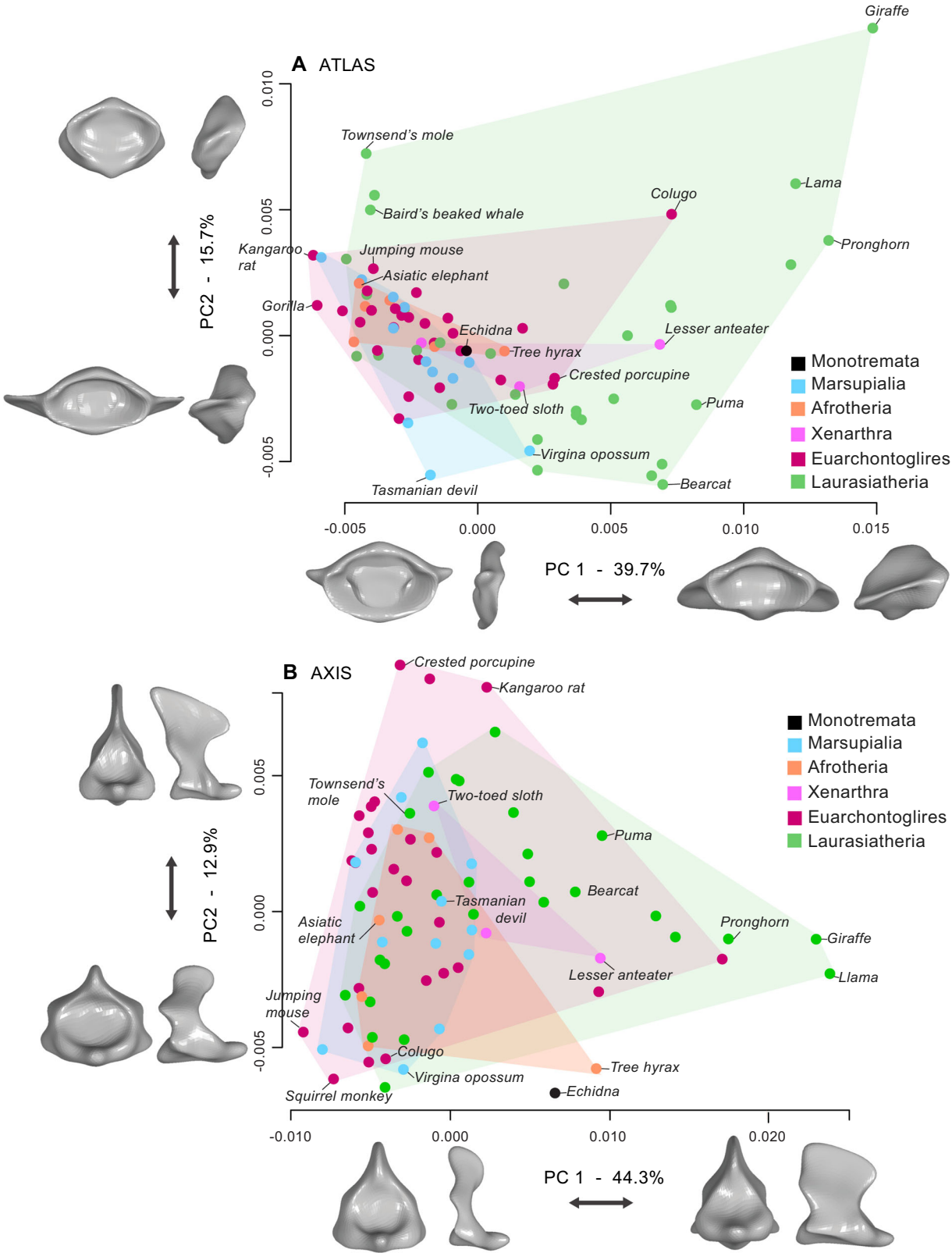

Figure 2. Morphospace plots showing the first two PC axes summarizing SPHARM coefficients for (A) atlas and (B) axis shape across mammals. Convex hulls illustrate morphospace occupation by different subclades. 3D mesh eigenshapes representing ±2 standard deviations of each PC axis are shown in cranial and lateral view.

scores for the atlas and axis across different diet and locomotor groups, including plots of the original PC scores as well as the residuals of PC scores regressed on $\log_{10}$-body mass (Fig. 3). These plots are illustrative and do not contain information on significance of shape differences between groups, because we opted to use an information-theoretic approach rather than null-hypothesis significance testing (Burnham et al. 2011). Linear regression coefficients of PC scores on $\log_{10}$-body mass and scatterplots of PC scores versus body mass are presented in Table S6 and Fig. S2.

Results

ATLAS AND AXIS MORPHOSPACES

PC1 of atlas shape primarily describes changes in the craniocaudal length of the vertebra and the orientation of the transverse processes (Fig. 2A). Species with low PC1 scores tend to have short, craniocaudally compressed vertebral arches and proportionally narrow, horizontally oriented transverse processes, whereas species with high PC1 scores have craniocaudally longer atlases and somewhat caudally rotated transverse processes. Most species in our analyses have low PC1 scores, but a few euarchontoglirans (e.g., the gliding colugo) and many laurasiatheres (particularly ungulates) exhibit positive PC1 scores. PC2 of atlas shape mainly describes changes in the dorsoventral height of the vertebral arch and the lateral extension of the transverse processes. Species with negative PC2 scores have laterally extended transverse processes and more dorsoventrally compressed vertebral arches, whereas species with positive PC2 scores have reduced transverse processes and relatively taller vertebral arches (Fig. 2A).

The axis morphospace reveals patterns of shape variation similar to those observed in the atlas. PC1 of axis shape is strongly influenced by the craniocaudal length of the dens, centrum, vertebral arches, and spinous process, all of which increase along PC1 (Fig. 2B). Axis PC2 describes changes in the dorsoventral height, craniocaudal length, and angle of the spinous process, as well as changes in the dorsoventral height and mediolateral width of the vertebral arches. Species with negative PC2 scores have wide, dorsoventrally compressed vertebral arches and short, anteriorly projecting or nonangled spinous processes; species with positive PC2 scores have narrower vertebral arches and taller, more steeply angled spinous processes (Fig. 2B).

Although species positions within the atlas and axis morphospaces are roughly equivalent along PC1 (corresponding to craniocaudal length in both vertebrae), species are more evenly scattered across PC2 in the axis morphospace than in the atlas morphospace. In the latter, a few laurasiatherian species (e.g., giraffe, llama, and Baird's beaked whale) have high PC2 scores, whereas most other species are concentrated near the origin or toward low PC2 scores.

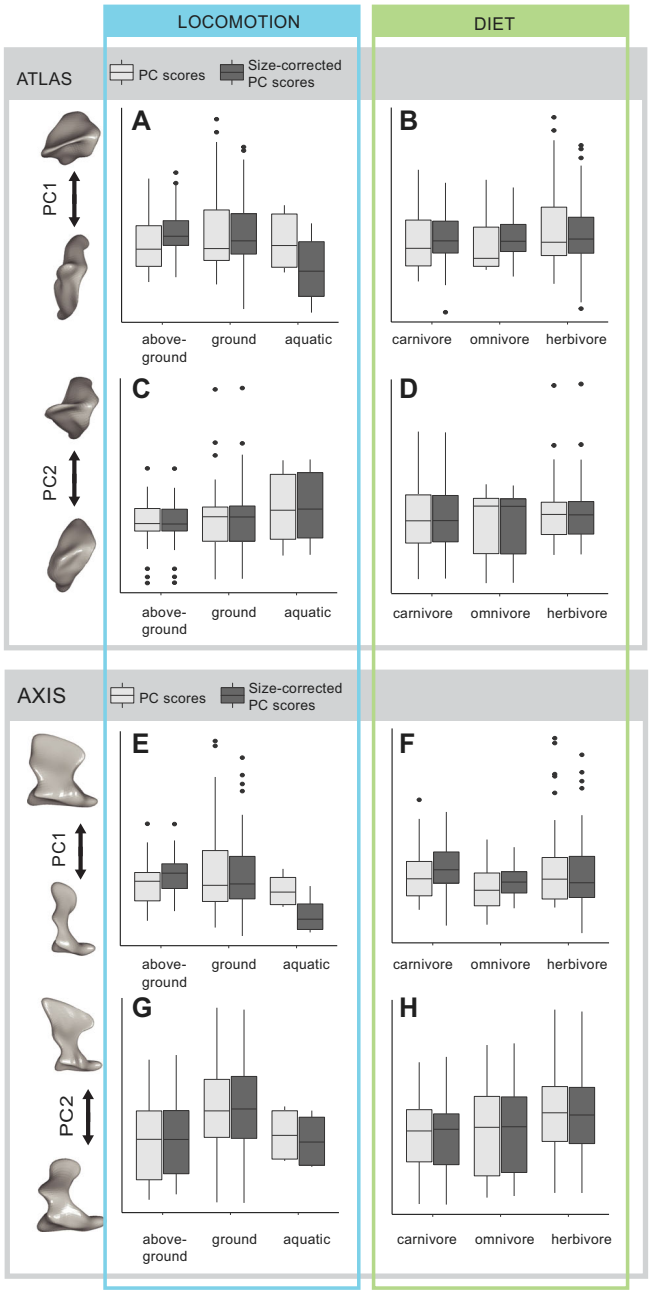

Figure 3. Box plots showing the relationship between locomotion and shape (A, C, E, and G) and diet category and shape (B, D, F, and H) for atlas and axis vertebrae. Light gray boxes represent PC scores, whereas dark gray boxes represent size-corrected residuals obtained from a linear regression of PC scores on $\log_{10}$ body mass (see Table S4 for regression coefficients). Eigenshapes representing the extreme vertebra shapes of each PC are shown in lateral view. These plots are intended to illustrate trends from the PGLS analyses and do not contain information on statistical significance. Dots above and below boxes represent outliers.

Table 1. Multivariate disparity of atlas and axis shape between mammalian subclades, measured as the Procrustes variance in all 80 PCs between groups using the *morphol.disparity* function in the geomorph R package.

Subclade	No. of families	No. of families sampled	Percentage sampled	Estimated divergence time (million years ago)	Atlas Procrustes variance	Axis Procrustes variance
Laurasiatheria	69	31	45	84.6	8.668×10^{-5}	1.445^{-4}
Euarchontoglires	52	27	52	83.3	3.854×10^{-5}	7.642×10^{-5}
Marsupialia	24	12	50	81.8	3.861×10^{-5}	6.999×10^{-5}
Afrotheria	12	6	50	80.9	3.425×10^{-5}	6.663×10^{-5}
Xenarthra	5	3	60	65.4	4.339×10^{-5}	1.178×10^{-4}
Monotremata	2	1	50	36.7	N/A	N/A

Atlas pairwise disparity was significantly different between Laurasiatheria and Euarchontoglires ($P = 0.001$) and Laurasiatheria and Marsupialia ($P = 0.03$); axis pairwise disparity was significantly different between Laurasiatheria and Euarchontoglires ($P = 0.009$) and Laurasiatheria and Marsupialia ($P = 0.038$); no other between-group comparisons were significant ($P > 0.05$). Sampling coverage of families within each superorder is included, as well as estimated divergence time (from Meredith et al. 2011).

In both the atlas and axis datasets, PC1 and PC2 exhibit K statistics significantly different from 0 (and see Table S7 for the rest of the PCs), indicating phylogenetic signal in the shape data (Blomberg et al. 2003). Inspection of the atlas and axis morphospaces reveals that laurasiatherian mammals occupy larger portions of morphospace than other groups (Fig. 2). The multivariate shape disparity, measured as the Procrustes variance in all PCs among groups, was highest in Laurasiatheria for both atlas and axis vertebrae (Table 1). Among the six subclades, atlas and axis pairwise disparity was significantly different between Laurasiatheria and Euarchontoglires, and between Laurasiatheria and Marsupialia (Table 1). Although some subclades were represented by fewer species, our sample represented 45–60% of the family-level diversity within each group regardless of taxonomic diversity (as determined by Meredith et al. 2011).

PREDICTORS OF ATLAS SHAPE DIVERSITY

The best-supported model predicting atlas shape variation along PC1 included both body mass and locomotion. However, a slightly more complex model including body mass, locomotion, and diet was similarly well supported (ΔAICc = 2.61; Table 2A). Taken together, these two models comprise 90% of the AICc weight. Plots of size-corrected atlas PC1 show relatively lower residuals in aquatic taxa than species that locomote on the ground and above ground, indicating relatively more craniocaudally compressed vertebral bodies and transverse processes in aquatic lineages (Fig. 3A). For atlas PC2 regressions, the model with the lowest AICc score included only the intercept and no other variables, but three additional models were similarly supported (Table 2B). Thus, changes in the mediolateral width of the vertebral arches and transverse processes, represented by PC2, were not clearly associated with particular ecological categories (Fig. 3C, D). Atlas morphology (PC1 and PC2) did not exhibit marked trends across diet categories (Fig. 3B, D).

PREDICTORS OF AXIS SHAPE DIVERSITY

Axis shape variation along PC1 is best explained by a model that includes both body mass and locomotion as predictors, but two other models (one including body mass, locomotion, and diet; one including only body mass) had similar explanatory power (Table 2C). Together, these three models comprised 90% of the AICc weight among all models. Size-corrected PC1 scores of aquatic taxa were relatively lower than those of above-ground and ground taxa, indicating more craniocaudally compressed vertebral arches, centra, and spinous processes in these species (Fig. 3E).

The best supported model explaining axis shape variation along PC2 includes locomotion as the only predictor, but is closely followed by models including both locomotion and diet, and body mass and locomotion (Table 2D). Thus, we found no clear trend in variation in axis PC2 with respect to specific predictors. Conversely, raw and size-corrected values of axis PC2 are slightly larger in ground taxa than above-ground and aquatic taxa (albeit exhibiting large variation). This suggests that some species that locomote on the ground have mediolaterally wider vertebral bodies, and dorsoventrally taller and craniocaudally lengthened spinous processes (Fig. 3G). As in the atlas, both size-corrected and raw axis PC1 and PC2 scores do not seem to differ among dietary categories (Fig. 3F, H).

In general, both the atlas and axis are more craniocaudally compressed in smaller mammals than in larger mammals, and larger mammals exhibit greater variation in shape (e.g., very high PC1 scores in the giraffe, and low PC1 scores in the elephant and whale; Fig. 2; see Fig. S2 for PC vs. body size plots).

Table 2. Aikaike information criterion (AICc) scores for phylogenetic generalized least squares (PGLS) regressions of ecomorphological variables (body mass, locomotion, and diet) on (A) atlas PC1, (B) atlas PC2, (C) axis PC1, and (D) axis PC2.

(A) Atlas PC1						
Model	df	AICc	ΔAICc	Akaike weight	ML lambda	Lambda 95% CI
Log mass + locomotion	7	−683.3	0	0.71	0.97	0.80, NA
Log mass + locomotion + diet	9	−680.7	2.61	0.19	0.97	0.80, NA
Log mass + diet	4	−677.5	5.75	0.04	0.99	0.85, NA
Log mass	2	−676.7	6.61	0.03	1.0	0.88, NA
Diet	3	−676.2	7.09	0.02	1.0	0.86, NA
Locomotion + diet	8	−672.9	10.43	0.00	1.0	0.89, NA
Intercept	1	−671.4	11.90	0.00	1.0	0.93, NA
Locomotion	6	−669.9	13.39	0.00	1.0	0.92, NA
(B) Atlas PC2						
Intercept	1	−710.9	0	0.43	0.74	0.38, 0.93
Log mass	2	−709.8	1.11	0.25	0.75	0.41, 0.93
Log mass + locomotion	7	−707.8	3.12	0.09	0.76	0.48, 0.93
Locomotion	6	−707.7	3.25	0.09	0.76	0.46, 0.93
Diet	3	−707.5	3.37	0.08	0.77	0.42, 0.94
Log mass + diet	4	−706.1	4.82	0.04	0.77	0.43, 0.94
Locomotion + diet	8	−703.3	7.61	0.01	0.78	0.47, 0.94
Log mass + locomotion + diet	9	−703.2	7.71	0.01	0.76	0.46, 0.93
(C) Axis PC1						
Log mass + locomotion	7	−576.7	0	0.52	0.73	0.14, 0.98
Log mass + locomotion + diet	9	−575.5	1.16	0.29	0.73	NA, 0.98
Log mass	2	−573.1	3.51	0.09	0.75	0.18, 1.0
Log mass + diet	4	−570.9	5.70	0.03	0.77	0.22, NA
Diet	3	−570.3	6.31	0.02	0.84	0.49, NA
Locomotion + diet	8	−570.3	6.39	0.02	0.84	0.51, NA
Intercept	1	−569.0	7.69	0.01	0.86	0.50, NA
Locomotion	6	−568.2	8.48	0.01	0.86	0.51, NA
(D) Axis PC2						
Locomotion	6	−655.2	0	0.34	0.52	NA, 0.95
Intercept	1	−653.5	1.65	0.15	0.62	NA, 0.97
Locomotion + diet	8	−653.5	1.71	0.14	0.62	NA, 0.98
Diet	3	−653.1	2.11	0.12	0.68	NA, NA
Log mass + locomotion	7	−652.8	2.41	0.10	0.522	NA, 0.95
Log mass	2	−652.1	3.04	0.07	0.62	NA, 0.97
Log mass + locomotion + diet	9	−651.1	4.09	0.04	0.62	NA, 0.99
Log mass + diet	4	−650.8	4.33	0.04	0.68	NA, NA

Column headings: model = predictor variables; df = degrees of freedom; AICc = AIC score corrected for small sample sizes; ΔAICc = difference in AICc score between a particular model and the model with lowest AICc value; Akaike weight = relative likelihood of model; ML lambda = maximum-likelihood estimate of Pagel's lambda for the PGLS model; Lambda 95% CI = 95% confidence interval of lambda value estimate.

Discussion

We present the first study examining the morphological diversity of the atlas–axis complex, an anatomical innovation that enabled mammals to achieve and specialize on ecologically important behaviors (Evans 1939; Kemp 1969; Crompton and Jenkins 1973). Using 3D imaging and high-dimensional analytical tools, we describe trends in morphological diversity across a taxonomically broad sample of extant mammals and examine the potential ecological drivers of this diversity. We found that shape disparity of both atlas and axis vertebrae varies across major clades and is greater in laurasiatherian mammals (Table 1). This is consistent with adaptive scenarios explaining the evolution of these skeletal

elements, as Laurasiatheria comprises an eclectic array of species, from bats to whales to horses, which are highly diverse in many ecological and physical aspects. Moreover, the lower disparity in vertebral shape in the most speciose clade, Euarchontoglires, highlights the possibility that morphological diversity in the cervical spine can be decoupled from species diversity in mammals (i.e., as previously described in mammalian body size, Venditti et al. 2011; squirrel jaw shape, Zelditch et al. 2015; and baleen whale morphology, Marx and Fordyce 2015).

We found some support for our hypothesis that atlas and axis shape diversity can be explained by ecomorphological factors such as body size, locomotion, and possibly diet. We also found evidence for the influence of past evolutionary history on the shape variation of these vertebrae, which is consistent with previous comparative studies of mammalian cranial (Marroig and Cheverud 2001; Raia et al. 2010; Goswami et al. 2011), appendicular (Polly 2008; Martín-Serra et al. 2015), and axial (Randau et al. 2016a) structures at large phylogenetic scales. Previous quantitative analyses indicated that primate atlas shape is associated with locomotion when phylogenetic history is ignored (Manfreda et al. 2006), but a more recent study in felids found that phylogeny influences cervical vertebra shape more than diet or locomotion (Randau et al. 2016a). The atlas articulates tightly with the base of the cranium, and the shape of this region exhibits strong phylogenetic signal in several groups of primates (Cardini and Elton 2008; Gilbert 2011) and carnivorans (Goswami 2006; Figueirido et al. 2010). If this is the case for other mammals, atlas shape may be generally constrained by this articulation, which is important for head flexion and extension, and could subsequently influence axis shape (Evans 1939).

Our analyses revealed an association between some aspects of atlas and axis shape and body size, such that smaller species tend to have craniocaudally compressed atlases and axes, whereas larger species show more variation in atlas and axis craniocaudal length. Therefore, scaling may be one of the mechanisms underlying variation in atlas and axis morphology across lineages. Previous studies of the axial skeleton within mammal orders and families support this idea. For example, the shape of the atlas in primates scales allometrically with body size, and larger primate species possess disproportionally thicker and more robust vertebral arches than smaller species (Manfreda et al. 2006). In felids, the atlases of larger bodied species display relatively longer ventral arches and taller centra (positively allometric), but relatively narrower prezygophyseal distance (negatively allometric) (Randau et al. 2016b). In bovids, larger species have proportionally (isometrically) longer centra of the lumbar vertebrae, but disproportionally (positively allometric) wide centra that may restrict flexion and extension at the lumbosacral joint (Halpert et al. 1987). Although body mass is a predictor in our best supported models for PC1 of both the atlas and axis, this relationship is nuanced. Smaller species tend to have short, compressed cervical vertebrae, but some large species, such as the Baird's beaked whale and Asiatic elephant, also exhibit relatively compressed vertebrae even at massive body sizes. Conversely, other large species, such as the giraffe, llama, and elk, have a relatively long atlas and axis for their size (Fig. S2). Therefore, atlas and axis length appears to be more variable among large-bodied taxa than small-bodied taxa. These results are consistent with a study of neck length modification in mammals, which found greater variation in the overall length of the cervical spine in larger species (Arnold et al. 2017).

Cervical vertebra count is remarkably consistent and developmentally constrained in mammals (Narita and Kuratani 2005; Asher et al. 2011), totaling seven vertebrae except in two sloth genera (*Bradypus* and *Choleopus*) (Hautier et al. 2010) and manatees (*Trichechus*) (Buchholtz et al. 2014). The tight constraint on cervical vertebra number may be due to the involvement of Hox genes responsible for cervical patterning in other developmental functions, as homeotic transformations of these elements are associated with major congenital abnormalities and cancer incidence in humans (Galis 1999; Galis et al. 2006). Further evidence has linked constraints in cervical count to the development and muscularization of the diaphragm (Buchholtz et al. 2012). With these meristic and homeotic constraints in the number of cervical vertebrae, the diversity of neck morphologies in mammals is achieved largely via homologous variation in the size and shape of the vertebrae, likely involving regionally expressed growth factors (Buchholtz 2012). It remains unclear what developmental mechanisms determine the length and width of individual vertebrae, but our results illustrate that, while very small mammals tend to have compressed atlases and axes, large mammals have evolved both long and short neck vertebrae in spite of their constrained cervical count. Therefore, the study of vertebrae developmental patterns and mechanisms in large mammals could prove more fruitful for understanding the intrinsic sources of vertebrae morphological diversity.

In addition to body size, our analyses revealed associations between atlas and axis shape and locomotor modes, although these relationships differed between the two vertebrae. This is not unexpected given the divergent functions of the atlas (supporting, flexing, and extending the head) versus the axis (rotation of the head about the neck) (Evans 1939). Importantly, our models supported an association between atlas and axis PC1 and locomotion when body mass was included as a covariate, but not when body mass was excluded (Table 2A and C). Smaller and larger species differ in their shape diversity, and our PGLS results indicate that the relationship between morphology and locomotor ecology may be confounded by the effect of body size. Comparisons of size-corrected atlas and axis PC1 scores across locomotor categories suggest that aquatic taxa have craniocaudally shorter, more compressed vertebrae than above-ground and ground-dwelling taxa

(Fig. 3A, E). This shortening of the cervical vertebrae has been considered an adaptation to aquatic life in cetaceans and manatees, in which a shorter neck reduces flexibility and decreases drag during swimming (Reidenberg 2007).

We found little support for the hypothesis that atlas and axis shape is associated with diet in mammals. PGLS models that included only diet, or diet in addition to body mass, were not among the best supported models predicting any set of PC scores for either the atlas or axis (Table 2). Boxplots of atlas and axis PC scores showed no discernable trend in shape variation across diet categories (Fig. 3B, D, F, and H). When highly supported models included diet as a predictor, it was always in addition to locomotion (Table 2A, C, and D). These results suggest that the effects of feeding behaviors on atlas and axis shape evolution, if any, may be surpassed by locomotor specializations.

Because this study explores shape variation in the atlas and axis at a broad taxonomic scale, our analyses of the relationship between morphology and ecological traits were similarly broad in scope. Realistically, mammals exhibit much greater ecological and functional diversity than what is captured by the categories employed here. However, dividing our sampled taxa into finer-scale categories, such as gliding or fossorial locomotion groups, would have led to insufficient sampling of each category to perform robust statistical analyses. Further, morphospace plots coded by locomotor mode illustrate that locomotor specialists such as gliders are not outliers in atlas and axis shapes (Fig. S3). We anticipate that the broad-scale trends presented here will provide a useful starting point to discern the complicated interplay of factors that may influence the evolution of vertebral shape in specific mammal orders. For example, future studies could focus on differences between carnivores that consume invertebrate versus vertebrate prey (Van Valkenburgh 1985), or species that dig with their forelimbs versus teeth (Lessa et al. 2008)—each of which may have different functional implications for the shape of the cervical vertebrae. Likewise, in species with horns or antlers, atlas and axis morphology may be under selection to accommodate muscles and ligaments involved in supporting the weight of these cranial structures and deploying them as weapons in intraspecific combat or predator defense (Stankowich 2012).

Conclusions

This study is the first to quantify the morphological diversity of the atlas–axis complex across mammals. Despite developmental constraints on cervical number, atlas and axis shapes are remarkably diverse across the mammals in our sample. In explaining this diversity, we found strong support for phylogenetic and scaling effects, moderate support for specialization for locomotion styles, and no apparent effect of broadly defined dietary categories. Our results highlight that the evolution of body size and locomotor behavior may have imposed different mechanical demands on the necks of mammals, influencing the morphological evolution of their atlas–axis complex.

AUTHOR CONTRIBUTIONS

A.V.L. performed CT and laser scans, conducted the SPHARM analyses and data analysis, and made the figures. K.C. cleaned 3D meshes, compiled ecological data from literature, and assisted with SPHARM analyses. E.B. performed laser scans and cleaned 3D meshes. S.E.S. designed the study and assisted with data analysis. All authors contributed to writing the manuscript and gave final approval for publication.

ACKNOWLEDGMENTS

We thank J. Bradley and volunteers at the Burke Museum of Natural History and Culture, Seattle, WA, for assisting with specimen use; M. McPeek for kind assistance with the spherical harmonics software SPHARM; J. Campbell for Matlab assistance and troubleshooting; members of the Santana Lab for helpful input during data collection and analysis; and D. Irschick for insightful feedback on the manuscript. This study was supported by the University of Washington's Department of Biology via startup funds to S.E.S.; A.V.L. received support from NSF GRFP award 1451512 while conducting this research.

DATA ARCHIVING

Supporting Information includes seven tables, three figures, supplemental references, and can be found with this article online. R code for analyses, raw data, and 3D models of vertebrae can be found in Dryad repository https://doi.org/10.5061/dryad.1nq8md7.

LITERATURE CITED

Adams, D. C., and E. Otárola-Castillo. 2013. Geomorph: an R package for the collection and analysis of geometric morphometric shape data. Methods Ecol. Evol. 4:393–399.

Arnold, P., E. Amson, and M. S. Fischer. 2017. Differential scaling patterns of vertebrae and the evolution of neck length in mammals. Evolution 71:1587–1599.

Asher, R. J., K. H. Lin, N. Kardjilov, and L. Hautier. 2011. Variability and constraint in the mammalian vertebral column. J. Evol. Biol. 24:1080–1090.

Bartoń, K. 2016. MuMIn: multi-model inference. Available at http://r-forge.r-project.org/projects/mumin/.

Blomberg, S. P., T. Garland, and A. R. Ives. 2003. Testing for phylogenetic signal in comparative data: behavioral traits are more labile. Evolution 57:717–745.

Buchholtz, E. A. 2012. Flexibility and constraint: patterning the axial skeleton in mammals. Pp. 230–256 *in* R. J. Asher and J. Muller, eds. From clone to bone: the synergy of morphological and molecular tools in paleobiology. Cambridge Univ. Press, New York.

Buchholtz, E. A., H. G. Bailin, S. A. Laves, J. T. Yang, M.-Y. Chan, and L. E. Drozd. 2012. Fixed cervical count and the origin of the mammalian diaphragm. Evol. Dev. 14:399–411.

Buchholtz, E. A., K. L. Wayrynen, and I. W. Lin. 2014. Breaking constraint: axial patterning in *Trichechus* (Mammalia: Sirenia). Evol. Dev. 16:382–393.

Burnham, K. P., D. R. Anderson, and K. P. Huyvaert. 2011. AIC model selection and multimodel inference in behavioral ecology: some background, observations, and comparisons. Behav. Ecol. Sociobiol. 65:23–35.

Cardini, A., and S. Elton. 2008. Does the skull carry a phylogenetic signal? Evolution and modularity in the guenons. Biol. J. Linn. Soc. 93:813–834.

Cardini, A., and P. D. Polly. 2013. Larger mammals have longer faces because of size-related constraints on skull form. Nat. Commun. 4:1–7.

Caro, T. M., C. M. Graham, C. J. Stoner, and M. M. Flores. 2003. Correlates of horn and antler shape in bovids and cervids. Behav. Ecol. Sociobiol. 55:32–41.

Christiansen, P. 2002. Mass allometry of the appendicular skeleton in terrestrial mammals. J. Morphol. 251:195–209.

Clauss, M., T. Kaiser, and J. Hummel. 2008. The morphophysiological adaptations of browsing and grazing mammals. Pp. 47–88 *in* I. J. Gordon and H. H. T. Prins, eds. The ecology of browsing and grazing. Springer, Berlin, Germany.

Coombs, M. C. 1983. Large mammalian clawed herbivores: a comparative study. Trans. Am. Philos. Soc. 73:1–96.

Crompton, A. W., and F. A. Jenkins. 1973. Mammals from reptiles: a review of mammalian origins. Annu. Rev. Earth Planet. Sci. 1:131–155.

Du Toit, J. T. 1990. Feeding-height stratification among African browsing ruminants. Afr. J. Ecol. 28:55–61.

Evans, F. G. 1939. The morphology and functional evolution of the atlas-axis complex from fish to mammals. Ann. N. Y. Acad. Sci. 39:29–104.

Figueirido, B., F. J. Serrano-Alarcón, G. J. Slater, and P. Palmqvist. 2010. Shape at the cross-roads: homoplasy and history in the evolution of the carnivoran skull towards herbivory. J. Evol. Biol. 23:2579–2594.

Felice, R. N., and A. Goswami. 2018. Developmental origins of mosaic evolution in the avian cranium. PNAS 115:555–560.

Galis, F. 1999. Why do almost all mammals have seven cervical vertebrae? Developmental constraints, Hox genes, and cancer. J. Exp. Zool. 285: 19–26.

Galis, F., T. J. M. Van Dooren, J. D. Feuth, J. A. J. Metz, A. Witkam, S. Ruinard, M. J. Steigenga, and L. C. D. Wijnaendts. 2006. Extreme selection in humans against homeotic transformations of cervical vertebrae. Evolution 60:2643–2654.

Gilbert, C. C. 2011. Phylogenetic analysis of the African papionin basicranium using 3-D geometric morphometrics: the need for improved methods to account for allometric effects. Am. J. Phys. Anthropol. 144:60–71.

Goswami, A. 2006. Morphological integration in the carnivoran skull. Evolution 60:169–183.

Goswami, A., N. Milne, and S. Wroe. 2011. Biting through constraints: cranial morphology, disparity and convergence across living and fossil carnivorous mammals. Proc. R. Soc. B Biol. Sci. 278:1831–1839.

Gould, S. J. 1966. Allometry and size in ontogeny and phylogeny. Biol. Rev. 41:587–640.

Granatosky, M. C., P. Lemelin, S. G. B. Chester, J. D. Pampush, and D. Schmitt. 2014. Functional and evolutionary aspects of axial stability in euarchontans and other mammals. J. Morphol. 275:313–327.

Halpert, A. P., F. A. Jenkins, and H. Franks. 1987. Structure and scaling of the lumbar vertebrae in African bovids (Mammalia: Artiodactyla). J. Zool. London 211:239–258.

Hautier, L., V. Weisbecker, M. R. Sanchez-Villagra, A. Goswami, and R. J. Asher. 2010. Skeletal development in sloths and the evolution of mammalian vertebral patterning. Proc. Natl. Acad. Sci. USA 107:18903–18908.

Jenkins, F. A. 1960. The evolution and development of the dens of the mammalian axis. Anat. Rec. 164:173–184.

Johnson, S. E., and L. J. Shapiro. 1998. Positional behavior and vertebral morphology in atelines and cebines. Am. J. Phys. Anthropol. 105:333–354.

Jones, K. E., J. Bielby, M. Cardillo, S. A. Fritz, J. O'Dell, D. L. Orme, K. Safi, W. Sechrest, E. H. Boakes, C. Carbone, et al. 2009. PanTHERIA: a species-level database of life history, ecology, and geography of extant and recently extinct mammals. Ecology 90:2648.

Jungers, W. L. 1984. Aspects of size and scaling in primate biology with special reference to the locomotor skeleton. Am. J. Phys. Anthropol. 27:73–97.

Kemp, T. S. 1969. The atlas-axis complex of the mammal-like reptiles. J. Zool. London 159:223–248.

Kikuchi, Y., Y. Nakano, M. Nakatsukasa, Y. Kunimatsu, D. Shimizu, N. Ogihara, H. Tsujikawa, T. Takano, and H. Ishida. 2012. Functional morphology and anatomy of cervical vertebrae in *Nacholapithecus kerioi*, a middle Miocene hominoid from Kenya. J. Hum. Evol. 62:677–695.

Kissling, W. D., L. Dalby, C. Flojgaard, J. Lenoir, B. Sandel, C. Sandom, K. Trojelsgaard, and J.-C. Svenning. 2014. Establishing macroecological trait datasets: Digitalization, extrapolation, and validation of diet preferences in terrestrial mammals worldwide. Ecol. Evol. 4:2913–2930.

Kitchener, A. 1988. An analysis of the forces of fighting of the blackbuck (*Antilope cervicapra*) and the bighorn sheep (*Ovis canadensis*) and the mechanical design of the horn of bovids. J. Zool. 214:1–20.

Lessa, E. P., A. I. Vassallo, D. H. Verzi, and M. S. Mora. 2008. Evolution of morphological adaptations for digging in living and extinct ctenomyid and octodontid rodents. Biol. J. Linn. Soc. 95:267–283.

Manfreda, E., P. Mitteroecker, F. L. Bookstein, and K. Schaefer. 2006. Functional morphology of the first cervical vertebra in humans and nonhuman primates. Anat. Rec. - Part B New Anat. 289:184–194.

Marroig, G., and J. M. Cheverud. 2001. A comparison of phenotypic variation and covariation patterns and the role of phylogeny, ecology, and ontogeny during cranial evolution of new world monkeys. Evolution 55:2576–2600.

Martín-Serra, A., B. Figueirido, J. A. Pérez-Claros, and P. Palmqvist. 2015. Patterns of morphological integration in the appendicular skeleton of mammalian carnivores. Evolution 69:321–340.

Marx, F. G., and R. E. Fordyce. 2015. Baleen boom and bust: a synthesis of mysticete phylogeny, diversity and disparity. R. Soc. Open Sci. 2:140434.

McPeek, M. A., L. Shen, J. Z. Torrey, and H. Farid. 2008. The tempo and mode of three-dimensional morphological evolution in male reproductive structures. Am. Nat. 171:E158–E178.

McPeek, M. A., L. Shen, and H. Farid. 2009. The correlated evolution of three-dimensional reproductive structures between male and female damselflies. Evolution 63:73–83.

Meredith, R. W., J. E. Janečka, J. Gatesy, O. A. Ryder, C. A. Fisher, E. C. Teeling, A. Goodbla, E. Eizirik, T. L. L. Simão, T. Stadler, et al. 2011. Impacts of the Cretaceous Terrestrial Revolution and KPg extinction on mammal diversification. Science. 334:521–524.

Nalley, T. K., and N. Grider-Potter. 2017. Functional analyses of the primate upper cervical vertebral column. J. Hum. Evol. 107:19–35.

Narita, Y., and S. Kuratani. 2005. Evolution of the vertebral formulae in mammals: a perspective on developmental constraints. J. Exp. Zool. Part B Mol. Dev. Evol. 304:91–106.

Orme, D., R. Freckleton, G. Thomas, T. Petzoldt, S. Fritz, N. Isaac, and W. Pearse. 2013. caper: comparative analyses of phylogenetics and evolution in R.

Pagel, M. 1999. Inferring the historical patterns of biological evolution. Nature 401:877–884.

Pellis, S. M., and R. C. E. Officer. 1987. An analysis of some predatory behaviour patterns in four species of carnivorous marsupials (Dasyuridae), with comparative notes on the eutherian cat *Felis catus*. Ethology 75:177–196.

Pérez-Barbería, F. J., and I. J. Gordon. 1999. The functional relationship between feeding type and jaw and cranial morphology in ungulates. Oecologia 118:157–165.

Pierce, S. E., J. A. Clack, and J. R. Hutchinson. 2011. Comparative axial morphology in pinnipeds and its correlation with aquatic locomotory behaviour. J. Anat. 219:502–514.

Polly, P. D. 2008. Adaptive zones and the pinniped ankle: a three-dimensional quantitative analysis of carnivoran tarsal evolution. Pp. 167–196 *in* E. J. Sargis and M. Dagosto, eds. Mammalian evolutionary morphology. Springer, Dordrecht, The Netherlands.

Popowics, T. E., and M. Fortelius. 1997. On the cutting edge: tooth blade sharpness in herbivorous and faunivorous mammals. Ann. Zool. Fennici 34:73–88.

R Core Team. 2018. R: a language and environment for statistical computing. R Foundation for Statistical Computing, Vienna, Austria.

Raia, P., F. Carotenuto, C. Meloro, P. Piras, and D. Pushkina. 2010. The shape of contention: adaptation, history, and contingency in ungulate mandibles. Evolution 64:1489–1503.

Randau, M., A. R. Cuff, J. R. Hutchinson, S. E. Pierce, and A. Goswami. 2016a. Regional differentiation of felid vertebral column evolution: a study of 3D shape trajectories. Org. Divers. Evol., https://doi.org/10.1007/s13127-016-0304-4.

Randau, M., A. Goswami, J. R. Hutchinson, A. R. Cuff, and S. E. Pierce. 2016b. Cryptic complexity in felid vertebral evolution: shape differentiation and allometry of the axial skeleton. Zool. J. Linn. Soc. 178:183–202.

Reichman, O. J., and S. C. Smith. 1990. Burrows and burrowing behavior by mammals. Pp. 197–244 *in* H. H. Genoways, ed. Current mammalology. Plenum Press, New York.

Reidenberg, J. S. 2007. Anatomical adaptations of aquatic mammals. Anat. Rec. 290:507–513.

Revell, L. J. 2012. phytools: an R package for phylogenetic comparative biology (and other things). Methods Ecol. Evol. 3:217–223.

Santana, S. E., E. R. Dumont, and J. L. Davis. 2010. Mechanics of bite force production and its relationship to diet in bats. Funct. Ecol. 24:776–784.

Shapiro, L. J., and C. V. Simons. 2002. Functional aspects of strepsirrhine lumbar vertebral bodies and spinous processes. J. Hum. Evol. 42:753–783.

Slater, G. J., and A. R. Friscia. 2019. Hierarchy in adaptive radiation: a case study using the Carnivora (Mammalia). Evolution 73:524–539.

Sargis, E. J. 2001. A preliminary qualitative analysis of the axial skeletal of tupaiids (Mammalia, Scandentia): functional morphology and phylogenetic implications. J. Zool. 253:473–483.

Shen, L., H. Farid, and M. A. McPeek. 2009. Modeling three-dimensional morphological structures using spherical harmonics. Evolution 63:1003–1016.

Sidor, C. A. 2001. Simplification as a trend in synapsid cranial evolution. Evolution 55:1419–1442.

Stankowich, T. 2012. Armed and dangerous: predicting the presence and function of defensive weaponry in mammals. Adapt. Behav. 20:32–43.

Van Valkenburgh, B. 1985. Locomotor diversity within past and present guilds of large predatory mammals. Paleobiology 11:406–428.

Van Valkenburgh, B., and C. B. Ruff. 1987. Canine tooth strength and killing behaviour in large carnivores. J. Zool. London 212:379–397.

VanBuren, C. S., and D. C. Evans. 2016. Evolution and function of anterior cervical vertebral fusion in tetrapods. Biol. Rev. Camb. Philos. Soc. 92:608–626.

Vander Linden, A., B. P. Hedrick, J. M. Kamilar, and E. R. Dumont. 2019. Atlas morphology, scaling and locomotor behaviour in primates, rodents and relatives (Mammalia: Euarchontoglires). Zool. J. Linn. Soc. 185:283–299.

Venditti, C., A. Meade, and M. Pagel. 2011. Multiple routes to mammalian diversity. Nature 479:393–396.

Wilson, D. E., and D. M. Reeder, eds. 2005. Mammal species of the world: a taxonomic and geographic reference (Vol. 1). JHU Press, Baltimore.

Ydesen, K. S., D. M. Wisniewska, J. D. Hansen, K. Beedholm, M. Johnson, and P. T. Madsen. 2014. What a jerk: prey engulfment revealed by high-rate, super-cranial accelerometry on a harbour seal (*Phoca vitulina*). J. Exp. Biol. 217:2239–2243.

Zelditch, M. L., J. Li, L. A. P. Tran, and D. L. Swiderski. 2015. Relationships of diversity, disparity, and their evolutionary rates in squirrels (Sciuridae). Evolution 69:1284–1300.

Zsoldos, R. R., and T. F. Licka. 2015. The equine neck and its function during movement and locomotion. Zoology 118:364–376.

Associate Editor: A. Goswami
Handling Editor: Mohamed A. F. Noor

Supporting Information

Additional supporting information may be found online in the Supporting Information section at the end of the article.

Figure S1. Phylogenetic relationships of taxa in this study, pruned from the 2011 time-calibrated molecular family-level tree of mammals published by Meredith et al. [41].

Figure S2. Scatterplots illustrating the relationship between body size and shape for the atlas (A and B) and axis (C and D) vertebrae.

Figure S3. Morphospace plots showing PC1 and PC2 scores coded by primary locomotor behavior (see SI Table 1) for (A) atlas and (B) axis.

Supporting Information

Table S1. Catalogue information, taxonomic information, and ecological data for all study taxa.

Table S2. List of pruned tip labels from the family-level phylogeny published by Meredith et al. (see main text Ref. 41) with corresponding representatives from each family included in this study.

Table S3. Positions and descriptions of landmarks used for SHARM model registration (see main text Fig. 1B).

Table S4. Standard deviation and proportion of variance explained by each principal component for the atlas and axis vertebrae.

Table S5. Aikaike information criterion (AICc) scores for phylogenetic generalized least squares (PGLS) regressions of ecomorphological variables (body mass, locomotion, and diet) on Atlas PC1–PC5 (A–E) and Axis PC1–PC5 (F–J).

Table S6. Coefficients from linear regression of atlas and axis PC scores on log-transformed body mass.

Table S7. Phylogenetic signal in atlas and axis shape estimated using Blomberg's K statistic for the first two PC scores for each species (*phylosig* function in the phytools R package).